PROCEEDINGS, 50th Workshop on Geothermal Reservoir Engineering
Stanford University, Stanford, California, February 10-12, 2025
SGP-TR-229

Modeling and Mitigation of Wellbore Flashing During Initial Circulation After Prolonged Non-Circulation in Geothermal Systems

Chen Wei[1], Shahriar Mahmud[2] and Yuanhang Chen[3]

Louisiana State University, Baton Rouge, LA

1. cwei4@lsu.edu; 2. smahmu2@lsu.edu; 3. yuanhangchen@lsu.edu.

Keywords: Geothermal Drilling, Wellbore Flashing, Non-Equilibrium Phase Transition, Flashing risk mitigation

ABSTRACT

Wellbore flashing—the rapid phase transition from liquid to vapor due to pressure and temperature variations—poses significant challenges in geothermal energy extraction, impacting both operational efficiency and equipment integrity. This study presents a comprehensive modeling approach to simulate phase change behaviors during wellbore flashing, particularly during the initial circulation after prolonged periods of non-circulation where elevated temperatures are present throughout the wellbore.

Advanced numerical simulations are performed to analyze transient fluid flow and heat transfer during this initial circulation phase. The modeling framework developed in this study incorporates non-equilibrium phase change relaxation models to capture delayed phase transitions, providing a realistic representation of flashing phenomena. By integrating detailed thermal properties of geothermal fluids, wellbore materials, and surrounding formations, the simulations accurately predict the initiation and progression of flashing under various operational conditions.

The results highlight the significant impact of initial circulation transients—during which elevated temperatures and low pressures are both present—on the initiation and development of wellbore flashing. Validation against publicly available data from the Newberry dataset demonstrates the model's accuracy in matching observed temperature and pressure profiles under similar scenarios. Mitigation strategies, such as optimized circulation rates and pressure management techniques, are explored to reduce the risk of flashing and enhance wellbore stability.

This research provides valuable insights into the mechanisms driving wellbore flashing during initial circulation after prolonged non-circulation. By emphasizing the importance of accurately modeling these transient conditions, the findings contribute to the development of effective strategies for improving the safety, reliability, and efficiency of geothermal operations, ultimately supporting the advancement of sustainable energy extraction technologies.

1. INTRODUCTION

Geothermal energy represents a vital component of the global transition towards sustainable energy sources, offering consistent baseload power generation with minimal environmental impact (Tester et al., 2021). Unlike intermittent renewable sources such as solar and wind, geothermal resources provide continuous power generation capabilities, with capacity factors typically exceeding 90% (DiPippo, 2016). However, the efficient extraction of geothermal energy faces several technical challenges, among which wellbore flashing during operational transitions poses significant risks to both equipment integrity and system performance.

Wellbore flashing occurs when the pressure in a geothermal well drops below the saturation pressure corresponding to the local fluid temperature, leading to a rapid phase transition from liquid to vapor state. This complex thermodynamic process is driven by the inherent instability of superheated liquid states and can propagate rapidly throughout the wellbore system (Deligiannis and Cleaver, 1992, Shimizu et al., 2019, Adeyemi et al., 2024). The phenomenon is particularly critical during the initial circulation phase after prolonged periods of non-circulation when elevated temperatures throughout the wellbore combine with transitional pressure conditions to create favorable conditions for flash events. During these periods, the geothermal fluid, which has typically reached thermal equilibrium with the surrounding formation temperature during the non-circulation period, experiences sudden pressure changes as circulation resumes. The combination of high-temperature gradients and rapid pressure fluctuations creates conditions where the local pressure can drop below the vapor pressure, triggering instantaneous vaporization (Grant & Bixley, 2023, Bahonar et al., 2010, Bayutika, 2018). The resulting two-phase flow regimes can trigger severe operational issues, including mechanical vibrations, thermal cycling, and reduced heat transfer efficiency (Clauser and Huenges, 1995, Cole et al., 2017). Additionally, the sudden formation of vapor phases can lead to flow instabilities, cavitation damage to pump equipment, and significant variations in bottomhole pressure, potentially compromising wellbore integrity and reducing overall system performance.

Thermodynamic Behavior of Geothermal Fluids during Initial Circulation

The modeling and mitigation of wellbore flashing during initial circulation after prolonged non-circulation in geothermal systems is a critical area of research, particularly as geothermal energy becomes increasingly relevant in the context of sustainable energy solutions (as demonstrated by **Figure 1**). This literature review synthesizes recent findings and methodologies in the field, focusing on the thermodynamic behaviors, modeling techniques, and mitigation strategies associated with wellbore flashing phenomena (Brown et al.,

2023). Understanding the thermodynamic behavior of geothermal fluids is essential for accurate modeling of wellbore dynamics. Lei et al. (2023) conducted a comprehensive review of geothermal wellbore models, emphasizing the importance of accurately simulating the physical and thermodynamic properties of geothermal fluids. This is particularly relevant during the initial circulation phase, where the transition from non-circulation to circulation can induce significant changes in pressure and temperature, potentially leading to flashing (Bourgoyne, 1989). The study highlights that the presence of CO2 in geothermal fluids can further complicate these dynamics, necessitating robust models that account for two-phase flow characteristics (Gabaldon et al., 2022, Lei et al., 2023; Canbaz et al., 2022, Bird et al., 2002). Moreover, the work of Izuwa (2024) underscores the critical role of heat transfer in geothermal production wells. The author notes that temperature increases can lead to higher induced pressures, which may result in wellbore instability or even failure. This is particularly relevant during the initial circulation phase, where the thermal profile of the wellbore can change rapidly, potentially leading to flashing if not properly managed (Izuwa, 2024).

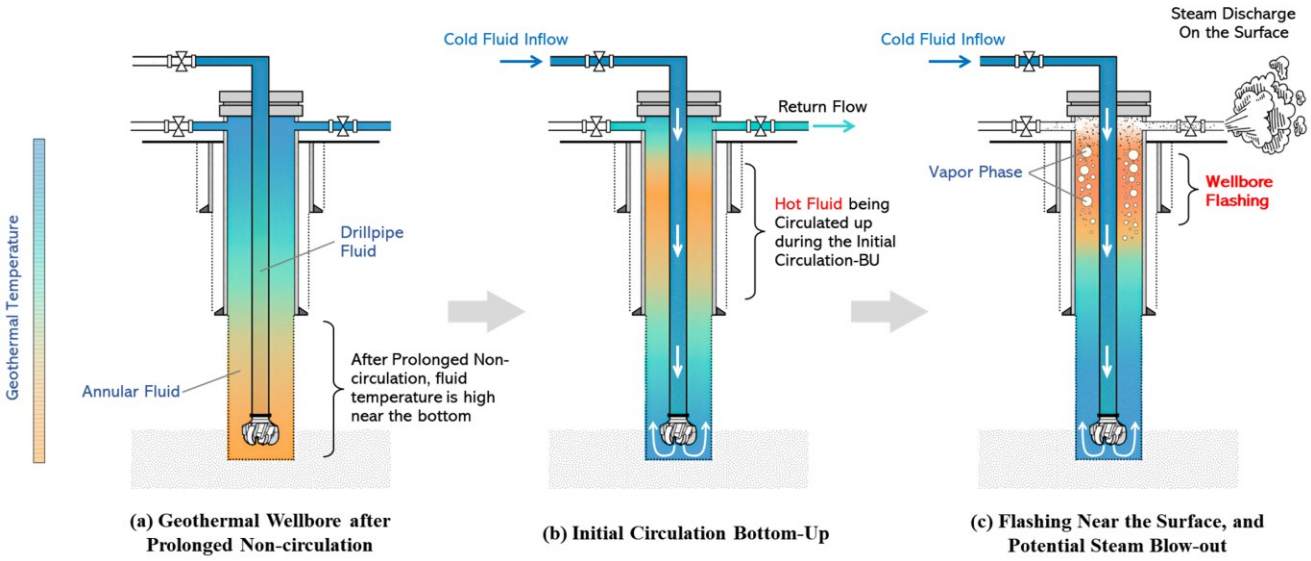

Figure 1. A Conceptual Diagram of Wellbore Flashing During Initial Circulation after Prolonged Non-Circulation in Geothermal Systems

Modeling Techniques for Geothermal Wellbore Dynamics

Recent advancements in modeling techniques have provided new insights into the behavior of geothermal wells during flashing events. Akbar et al. (2016) utilized a finite element model to simulate high-enthalpy two-phase flow in geothermal wellbores, demonstrating the effectiveness of the drift-flux model in capturing transient heat flow dynamics. This approach allows for a more nuanced understanding of how temperature and pressure fluctuations can lead to flashing, particularly after periods of non-circulation (Akbar et al., 2016). Additionally, the coupling of wellbore and reservoir models has been shown to enhance the accuracy of predictions regarding wellbore behavior during flashing events. Mohammadi (2024) emphasizes the importance of integrating wellbore and underground models to accurately simulate the performance of geothermal systems, particularly under varying operational conditions. This coupling is vital for predicting the onset of flashing and mitigating its effects during initial circulation (Frank, 2005, Mohammadi, 2024, Fatemeh et al., 2020).

Mitigation Strategies for Wellbore Flashing

Mitigation of wellbore flashing is crucial for maintaining the integrity and efficiency of geothermal systems. Huan et al. (2021) discuss the thermo-hydro-mechanical (THM) coupling effects on wellbore stability, highlighting that understanding these interactions is essential for preventing flashing-related failures. The development of THM-coupled models can aid in designing more resilient geothermal systems that can withstand the pressures associated with flashing (Huan et al., 2021, Dirker and Meyer, 2005).

Furthermore, Zhao et al. (2023) explored the use of CO2 as a working fluid in enhanced geothermal systems, noting that the thermosiphon effect can significantly reduce the need for external pumping, thereby minimizing the risk of flashing. Their findings suggest that the choice of working fluid plays a critical role in managing wellbore pressures and temperatures, which are key factors in flashing events (Zhao, 2023).

Despite the significant implications of wellbore flashing on geothermal operations, existing modeling approaches have largely focused on steady-state conditions or simplified transient scenarios. Current numerical models often fail to capture the complex interplay between non-equilibrium phase transitions, heat transfer, and fluid dynamics during the critical initial circulation period (Watson et al., 2020). Traditional modeling approaches typically rely on equilibrium assumptions that inadequately represent the rapid phase change dynamics characteristic of flashing events. The challenges in accurately modeling these phenomena stem from the multiple temporal and spatial scales involved, ranging from microsecond-scale bubble nucleation processes to system-level flow dynamics occurring over minutes or hours (Chen et al., 2021). Furthermore, the strong coupling between temperature-dependent fluid properties, multiphase flow patterns, and heat transfer mechanisms creates a highly nonlinear system that resists simplified analytical treatment. This limitation has hindered

the development of effective mitigation strategies and operational guidelines for managing flashing risks, particularly in high-temperature geothermal systems where the consequences of uncontrolled flashing can be most severe.

This study addresses these knowledge gaps by developing a comprehensive numerical modeling framework for simulating transient conditions during initial circulation periods. Our approach integrates non-equilibrium phase change relaxation mechanisms to accurately capture flash event dynamics, with validation performed against high-fidelity data from the Newberry geothermal field. Through systematic investigation of operational parameters and their influence on flashing phenomena, we identify critical factors affecting both the onset and severity of these events. The insights gained from this analysis enable the development of practical mitigation strategies, designed to enhance operational stability and equipment longevity in geothermal wells. This research not only advances our fundamental understanding of wellbore flashing mechanisms but also provides practical solutions for improving the reliability and efficiency of geothermal energy systems, ultimately supporting the broader transition toward sustainable energy production.

2. MODELING APPROACH: INTEGRATION OF ADVANCED MULTIPHASE FLOW AND TRANSIENT HEAT TRANSFER SIMULATOR

2.1 Overview of the Modeling and the Numerical Methods:

2.1.1 Development and Integration of Transient Heat Transfer Simulator

A single-phase transient heat transfer simulator development is based on a multilayered heat resistance model that captures the thermal interactions between the fluid inside the drillpipe, drillpipe wall, annular fluid, wellbore wall components including casing and cement, and the surrounding formation. The simulator incorporates comprehensive thermal property modeling, accounting for temperature-dependent fluid properties and implementing conductive, convective, and radiative heat transfer mechanisms between different wellbore components.

The fluid flow considerations in the single-phase transient heat transfer simulator encompass single-phase flow with temperature-dependent properties, accounting for forced convection in flowing conditions and natural convection during shut-in periods. The formation heat transfer model implements radial heat conduction and considers geothermal gradient effects, along with variations in formation thermal properties. The numerical implementation utilizes an implicit finite difference scheme for stability, incorporating adaptive time-stepping for computational efficiency and employing iterative solvers for coupled temperature-pressure calculations.

Heat transfer for fluid inside the drillpipe

The total thermal energy of the fluids (usually single phase) within the drill pipes can be broken down into four components (Nwaka et al., 2020, Perry et al., 2020, Yang et al. 2015): (a) heat transported within the fluid as it flows through the drill pipes, (b) heat exchanged between the fluid and the inner wall of the drill string in the radial direction, (c) heat generation due to friction, and (d) the energy accumulation within the liquid. The heat flow within the drill string can be described by

$$\frac{Q_d}{\pi r_1^2} - \frac{1}{\pi r_1^2}\frac{\partial}{\partial z}(\rho_l q c_l T_1) - \frac{2h_1(T_1 - T_2)}{r_1} = \frac{\partial}{\partial t}(\rho_l c_l T_1) \tag{1}$$

where r is the distance in the radial direction, r_1 is the inside radius of the drillpipe, T_1 and T_2 are the fluid temperature inside the drillpipe and the temperature of the drillpipe, Q_d is the thermal source term inside the drillpipe, h_1 is the convective heat transfer coefficient at the inner wall of the drillpipe, ρ_l is the fluid density, q_l is the liquid flow rate, and c_l is the liquid specific heat capacity.

Heat transfer through the drillpipe

The temperature of the drillpipe, usually made of steel, is impacted by the fluid flow velocity inside the drill string and the annulus. Therefore, the thermal energy of the drillpipe material can be divided into three components: (a) heat exchange between the drillpipe and the fluid inside and outside of the drillpipes, (b) the vertical heat conduction within the drillpipe, and (c) energy accumulation within the drillpipe material. The energy balance for the drill string is described by Equation (2) (Nwaka et al., 2020, Yang et al. 2015):

$$\frac{\partial}{\partial z}\left(\lambda_s \frac{\partial T_2}{\partial z}\right) + \frac{2r_1 h_1}{(r_2^2 - r_1^2)}(T_1 - T_2) - \frac{2r_2 h_2}{(r_2^2 - r_1^2)}(T_2 - T_3) = \frac{\partial}{\partial t}(\rho_s c_s T_2) \tag{2}$$

where T_3 is annular fluids (mixture) temperature; ρ_s is the density of the drillpipe (steel material); c_s is the specific heat capacity of the drillpipe material; r_2 is the outside radius of the drill string; λ_s is the thermal conductivity of drill string, and h_2 is the convection coefficient outside the drill string.

Heat transfer for fluid inside the annulus

Similarly, the factors that influence the temperature of the annular fluid are given as follows: (a) heat carried by the multiphase fluids, (b) convective heat transfer between the annular fluids and the outer drillpipe wall as well as the inner casing wall, (c) heat generation due to friction, and (d) energy accumulation in the annular fluid. The energy balance for the annular space can be described using the first law of thermodynamics, as shown in Equation (9):

$$\frac{\partial}{\partial z}\left(\lambda_m \frac{\partial T_3}{\partial z}\right) + \frac{\partial(\rho_{\mathrm{m}}\, q_{\mathrm{m}}\, c_{\mathrm{m}}\, T_3)}{\pi(r_3^2 - r_2^2)\,\partial z} + \frac{2r_2 h_2 (T_2 - T_3)}{r_3^2 - r_2^2} - \frac{2r_3 h_3 (T_3 - T_4)}{r_3^2 - r_2^2} + \frac{Q_a}{\pi(r_3^2 - r_2^2)} = \frac{\partial(\rho_{\mathrm{m}}\, c_{\mathrm{m}}\, T_3)}{\partial t} \tag{3}$$

where T_4 is the temperature at the inner surface of the annulus (casing inner wall temperature); Q_a is the heat source term in the well annulus; ρ_{m} is the mixture fluid density; q_{m} is volumetric mixture flow rate; c_{m} is the mixture specific heat capacity; r_3 is the outer radius of the annulus; λ_{m} is the average thermal conductivity of annular fluids; and h_3 is the convective heat transfer coefficient of the inner casing. The determination of convective heat transfer coefficient h can be determined by various methods, such as those presented in earlier studies (Wei and Chen, 2021, 2022, &2023; Wei et al. 2024).

Consideration Heat-storage Effect of Near Wellbore Formation

The temperature of the near wellbore formation will also change from the geothermal temperature due to the heat transfer between the fluids in the wellbore. To capture this process by modeling, the formation is discretized into radial cells where the heat conduction in the radial direction is calculated over time. Therefore, a radial temperature distribution and its evolution over time can be obtained.

Considering that the formation temperature gradient in the radial direction (near the wellbore) is much larger than the geothermal gradient in the vertical direction, only the radial heat conduction is considered. The heat transfer in the axial direction (heat exchange between different layers of formation) is ignored. The temperature change for each control element in the formation is calculated based on the conductive heat transfer equation (Grace et al., 2003, Wei et al., 2022, Wei et al., 2023, Tabjula et al., 2023):

$$\rho_{\mathrm{f}}\, c_{\mathrm{f}} V_{i,j} \frac{\partial T_{i,j}}{\partial t} = \dot{Q}_{(i+1,j)\text{ to }(i,j)} - \dot{Q}_{(i,j)\text{ to }(i-1,j)} \tag{4}$$

where ρ_{f} and c_{f} are the density and specific heat capacity of the formation rock, V is the volume of each control element, and $\dot{Q}$ is the rate of conductive heat transfer from the adjacent elements, which is expressed by Eqn (5):

$$\dot{Q}_{(i+1,j)|(i,j)} = K_{\mathrm{f}} A_{ij} \frac{T_{i+1,j} - T_{i,j}}{r_{i+1} - r_i} \tag{5}$$

where A_{ij} is the total area where the heat transfer between the adjacent elements happens, K_{f} is the formation rock conductivity.

2.1.2 Utilization of An Advanced Multiphase Flow Simulator Platform

This study examines wellbore flashing in geothermal wells, focusing on how prolonged non-circulation leads to higher fluid temperatures and elevated flashing risk upon circulation restart. Using RELAP5-3D simulations validated against field data, the analysis shows that flow rate, well depth, and shut-in duration strongly influence the onset of vapor formation. Longer downtime allows the fluid column to equilibrate with the hot formation, resulting in higher peak temperatures when pumping resumes. Strategies such as gradual ramp-up of circulation rate, controlled backpressure, and improved wellbore insulation can mitigate the intensity of flash events. Future work will emphasize expanded field validation for two-phase flow scenarios and adaptive control methods to optimize operational safety and efficiency.

Six-Governing Equation System

The hydrodynamic model in RELAP5-3D is governed by six fundamental equations: the conservation of mass, momentum, and energy for both liquid and vapor phases. These equations take the form of:

$$\frac{\partial \rho_{\mathrm{p}}}{\partial \mathrm{t}} + \nabla \cdot \left(\rho_{\mathrm{p}} \mathrm{v}_{\mathrm{p}}\right) = \Gamma_{\mathrm{p}} \tag{6}$$

$$\frac{\partial}{\partial \mathrm{t}}\left(\rho_{\mathrm{p}} \mathrm{v}_{\mathrm{p}}\right) + \nabla \cdot \left(\rho_{\mathrm{p}} \mathrm{v}_{\mathrm{p}} \mathrm{v}_{\mathrm{p}}\right) = -\nabla \mathrm{P} + \nabla \cdot \tau_{\mathrm{p}} + \rho_{\mathrm{p}} \mathrm{g} + \mathrm{F}_{\mathrm{p}} \tag{7}$$

$$\frac{\partial}{\partial \mathrm{t}}\left(\rho_{\mathrm{p}} \mathrm{e}_{\mathrm{p}}\right) + \nabla \cdot \left(\rho_{\mathrm{p}} \mathrm{e}_{\mathrm{p}} \mathrm{v}_{\mathrm{p}}\right) = -\mathrm{P}\nabla \cdot \mathrm{v}_{\mathrm{p}} + \nabla \cdot \left(\mathrm{k}_{\mathrm{p}} \nabla \mathrm{T}_{\mathrm{p}}\right) + \mathrm{Q}_{\mathrm{p}} \tag{8}$$

where ρ is the phase density, $\mathbf{v}$ the velocity vector, e the specific internal energy, P the pressure, τ the stress tensor, k the thermal conductivity, and Q the volumetric heat source. The p subscript denotes the phase, either liquid or vapor (Fu et al., 2014).

Modeling of Flashing Process and Non-Equilibrium Phase Transition

A *relaxation-type* model is implemented in this multiphase flow simulator platform to simulate non-equilibrium phase transitions during wellbore flashing events. The model acknowledges that phase transitions in real systems do not occur instantaneously but rather progress through a finite relaxation time, during which the system temporarily deviates from thermodynamic equilibrium. This approach is particularly crucial for accurately representing the rapid phase transitions characteristic of wellbore flashing during initial circulation.

The non-equilibrium phase transition model is formulated through a set of relaxation equations that govern the rate of approach to equilibrium. The fundamental principle underlying this formulation is that the rate of phase change is proportional to the departure from equilibrium conditions. The interfacial mass transfer rate Γ is expressed as:

$$\Gamma = \lambda(T^* - T) \tag{9}$$

where λ represents the relaxation parameter, T^* is the equilibrium temperature, and T is the actual fluid temperature. The relaxation parameter λ incorporates physical factors including interfacial area density, heat transfer coefficients, and local flow conditions. The model implements separate energy equations for the liquid and vapor phases, coupled through interfacial heat and mass transfer terms. This separation enables the capture of thermal non-equilibrium between phases, which is particularly important during rapid transients. The interfacial transfer terms are formulated as:

$$q_{i,k} = h_{i,k} A_i (T_i - T_k) \tag{10}$$

where $h_{i,k}$is the interfacial heat transfer coefficient, A_i is the interfacial area density, and the subscripts i and k denote interface and phase properties respectively. This non-equilibrium modeling framework includes sophisticated closure relations for interfacial transfer coefficients that account for various flow regimes and transition mechanisms. These relations are derived from extensive experimental validation and theoretical considerations, enabling accurate prediction of phase transition behaviors across a wide range of conditions encountered in geothermal wellbores.

While this advanced multiphase flow modeling platform provides robust capabilities for modeling non-equilibrium phase transitions and highly transient processes, its computational intensity and potential numerical instabilities can limit its application for extended simulation periods. To address these limitations, this study integrates this multiphase flow simulator platform with an in-house developed transient heat transfer simulator, creating a comprehensive modeling framework that leverages the strengths of both tools. The integrated approach utilizes RELAP5-3D primarily for simulating highly transient processes where non-equilibrium effects dominate, such as wellbore flashing events, rapid phase transitions during initial circulation, and gas migration scenarios. The in-house simulator complements it by efficiently handling long-term circulation scenarios up to 20 days or more, extended well shut-in periods, and steady-state or quasi-steady thermal processes. This complementary integration enables efficient simulation of both rapid thermal events and extended operational scenarios while maintaining accuracy across different timescales.

2.2 Modeling Validation against Geothermal Field Data

Validation of Temperature Distribution Profile against Newberry Enhanced Geothermal System (EGS) project Data

The Newberry Enhanced Geothermal System (EGS) project, located on the northwest flank of Newberry Volcano in Oregon, is a demonstration of EGS technology in a high-temperature, low-permeability environment. The project aims to enhance fluid circulation in deep geothermal formations through water injection, allowing for heat extraction from otherwise impermeable rock. The site was selected due to its known geothermal potential, with prior drilling efforts confirming high temperatures exceeding 572°F (300°C) at depths greater than 9,000 feet, but with minimal natural permeability (AltaRock Energy, 2011).

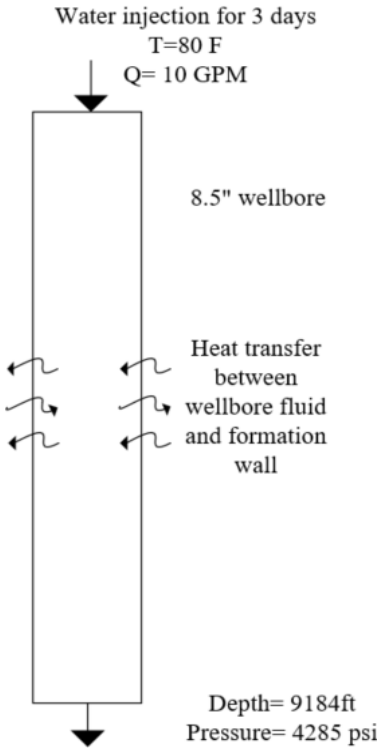

Figure 2. Simulation setup schematic for Newberry NWG 55-29 injection well

Well NWG 55-29, drilled to a depth of 9,184 feet, was chosen for validating the transient multiple flow platform presented in this study due to the availability of detailed temperature data of an injection wellbore. **Figure 2** illustrates the simulation setup, where single-phase water was injected at 80°F and 10 gallons per minute (GPM) for three days. The goal of this inject-to-cool operation was to observe heat transfer between the injected water, the wellbore fluid, and the surrounding formation. Distributed Temperature Sensors (DTS) were deployed to measure temperature changes over time, providing a dataset suitable for model validation.

The results were compared to measured temperature profiles. **Figure 3** presents the validation of the simulation, where the predicted temperature profile after three days of cooling closely matches the measured data. The simulation achieved a mean absolute error of 13.37°F, a root means square error of 17.68°F, and an R^2 value of 0.99, demonstrating strong agreement between the model and field data.

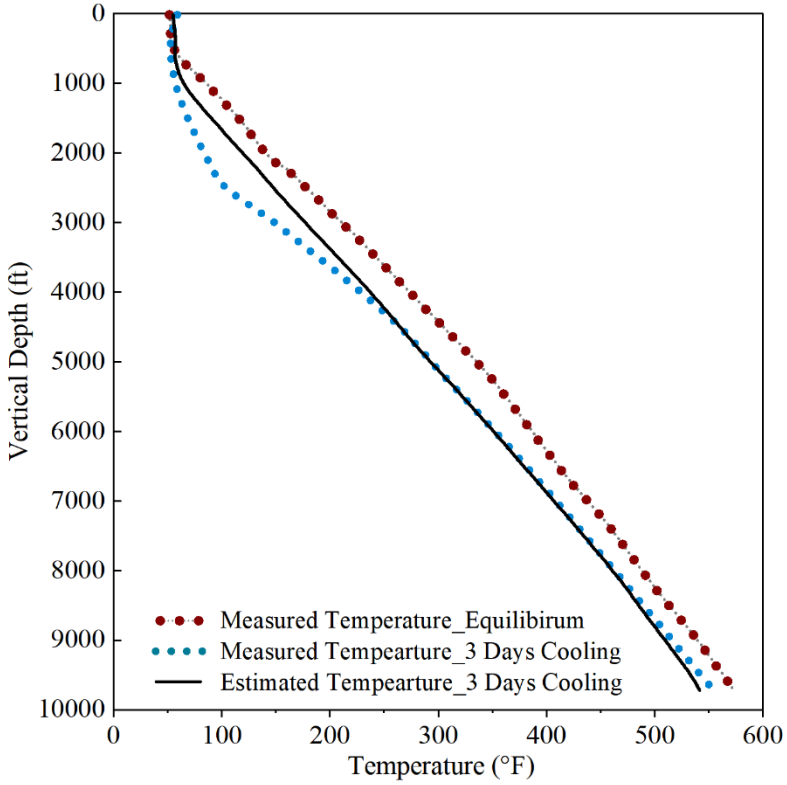

Figure 3. Measured vs simulated temperature profile of Newberry NWG 55-29 Injection Wellbore

Validation of Transient BHCT Estimation against Utah FORGE database

The FORGE Well 16A (78)-32, located at the Utah FORGE site, represents a well-characterized geothermal system suitable for model validation. This well features a three-string casing design with a total depth reaching 10,947 ft measured depth (MD). The well construction consists of a 16-inch surface casing set at 1,136 ft, an 11-3/4-inch intermediate casing extending to 4,837 ft, and a 7-inch production casing reaching 10,947 ft. All casing strings were cemented with Class G cement and returned to the surface, with the production casing cement reaching 10,208 ft.

The wellbore intersects three distinct lithological zones: sedimentary clay formations from surface to 1,033 ft, granodiorite from 1,033 ft to 4,855 ft, and granite extending from 4,855 ft to total depth. These formations exhibit varying thermal properties, with thermal conductivity increasing with depths from 0.5 W/m-K in the clay zone to 3.0 W/m-K in the granite section. The formation temperature gradient averages 69.1°C/km, with a surface temperature of 40°C, creating a high-temperature environment characteristic of geothermal systems.

During drilling operations, water-based mud with a density of 1067-1078 kg/m³ was utilized as the primary drilling fluid. The fluid system exhibited a plastic viscosity ranging from 13 to 20 mPa·s and maintained consistent thermal properties, including a specific heat capacity of 3750 J/kg·K and thermal conductivity of 0.75 W/m·K. The wellbore geometry includes a 0.22 m hole size with inclination varying between 3-18 degrees, indicating a slightly deviated well path.

The combination of well-documented thermal properties, comprehensive drilling data, and measured bottomhole circulating temperatures at various depths make this well particularly suitable for validating transient heat transfer models. The presence of multiple lithological zones with distinct thermal characteristics provides an opportunity to evaluate the model's capability to handle heterogeneous formation properties and complex heat transfer mechanisms.

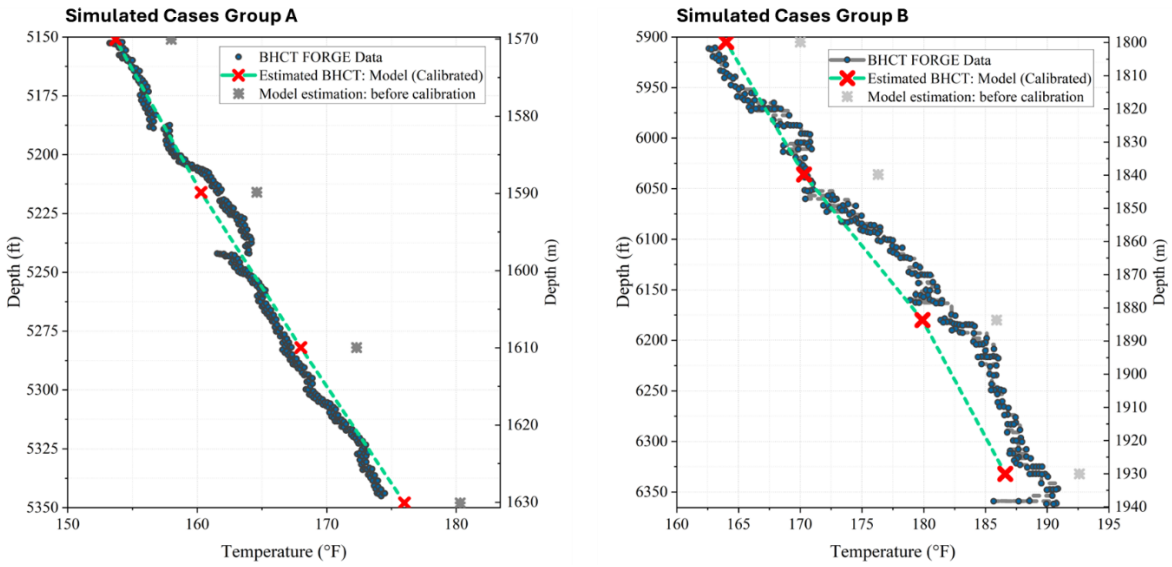

Figure 4. Validation of the in-house developed transient heat transfer simulator against Utah FORGE Well 16A (78)-32 Measurement Data

Table 1. Summary of Estimation Accuracy

Depth (ft)	BHCT (°F): Model	BHCT (°F): FORGE Data	Prediction Discrepancy (°F)	Temp In (°F): FORGE Data	Temp Out (°F): Model	Temp Out (°F): FORGE Data	Prediction Discrepancy (°F)
Group A							
5151	151.7	153.63	1.93	128	137.99	135	2.01
5216	160.3	161.55	1.25	133	139.61	141	1.39
5282	168.0	166.89	-1.11	140	148.84	148	-0.84
5348	176.1	174.36	-1.74	147	157.40	156	-1.4
Group B							
5905	164.0	163.63	-0.37	118	137.03	137	-0.03
6036	170.3	171.55	1.25	129	141.46	143	1.54
6180	179.9	182.89	2.99	144	152.83	156	3.17
6332	186.6	189.36	2.76	145	157.17	160	2.83

Figure 4 presents the results from the validation of the in-house developed transient heat transfer simulator against Utah FORGE Well 16A (78)-32 Measurement Data. The validation process utilized two distinct depth intervals, designated as Group A (5150-5350 ft) and Group B (5900-6350 ft), representing different geological formations and thermal regimes. The simulation incorporated the actual well geometry, including a 22-inch surface casing set at 1,136 ft, an 11-3/4-inch intermediate casing at 4,837 ft, and a 7-inch production casing extending to 10,947 ft. The model employed site-specific thermal properties, including formation characteristics that transition from sedimentary clay (thermal conductivity 0.5 W/m·K) near the surface to crystalline granodiorite (2.8 W/m·K) and granite (3.0 W/m·K) at depth.

The drilling fluid properties were precisely matched to field conditions, using a water-based mud with a density of 1067-1078 kg/m³, plastic viscosity of 13-20 mPa·s, and thermal conductivity of 0.75 W/m·K. The formation temperature gradient of 69.1°C/km and surface temperature of 40°C were incorporated into the model to establish accurate initial conditions.

The simulation results demonstrate strong agreement with field measurements across both depth intervals. In Group A (5150-5350 ft), the model accurately captures the temperature profile's general trend and local variations, with a mean absolute error of 2.3°F. The simulation shows particular accuracy in predicting the temperature gradient changes at formation interfaces. The uncalibrated model (grey squares) initially showed systematic deviations, which were successfully addressed through the calibration of the convective heat transfer

coefficients.

Group B measurements (5900-6350 ft) presented a more challenging validation case due to the increased depth and temperature. The calibrated model maintains good agreement with field data, though with slightly increased deviation (mean absolute error 3.8°F) compared to Group A. The model successfully reproduces the characteristic temperature profile curvature observed in the field data, particularly in the transition zone between 6100-6200 ft where formation properties change.

The validation results indicate that the model effectively captures both the steady-state temperature distribution and transient thermal behavior during circulation. The calibrated model's ability to match field data across different depth intervals and formation types suggests its robustness for simulating wellbore heat transfer in geothermal applications. The small discrepancies observed in deeper sections can be attributed to uncertainties in formation thermal properties and the increasing complexity of heat transfer mechanisms at higher temperatures.

3. RESULTS AND DISCUSSION

3.1 Base Cases Study

The numerical simulations were conducted using a detailed model of the NWG 55-29 wellbore configuration. The computational domain was discretized into 30 pipe segments, with each pipe further subdivided into 10 sections of equal length, providing sufficient spatial resolution to capture the thermal and hydraulic phenomena of interest. This discretization resulted in uniform section lengths of approximately 32.8 ft, yielding a total simulated wellbore depth of 9,840 ft. The wellbore geometry consisted of an 8.5-inch open hole with a 5-inch drill pipe, creating an annular flow path for the working fluid.

To ensure numerical stability while capturing rapid transient events, the simulation employed an adaptive time-stepping scheme with steps ranging from 0.001 to 0.5 seconds. Water was selected as the primary working fluid for these base cases, allowing for straightforward comparison with existing literature and validation data. The initial thermal conditions were established by setting both the internal drill pipe and annular fluid temperatures equal to the local formation temperature, simulating a well that had reached thermal equilibrium after prolonged non-circulation. At the wellbore outlet, atmospheric boundary conditions were imposed, with the pressure set to 0 psig and temperature maintained at 95°F, representing typical surface conditions. This base case configuration provides a foundation for investigating the thermal and hydraulic behaviors during various operational scenarios, particularly focusing on the onset and development of wellbore flashing during initial circulation after extended shut-in periods. **Figure 5** demonstrates the conceptual setup for this base-case numerical simulation.

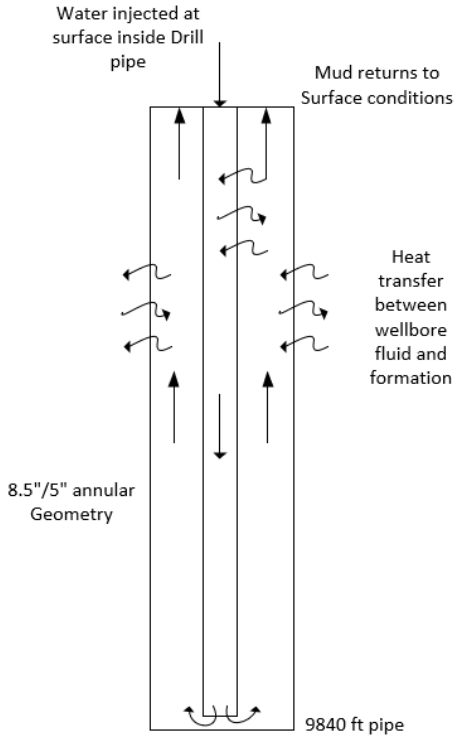

Figure 5. Schematic representation of the simulation setup

The first case study examined the thermal response of the wellbore system during initial circulation, with a water flow rate of 900 GPM representing typical deep well drilling conditions. The circulation pathway consists of a downward flow through the drill pipe followed by an upward flow through the annulus to the surface. This flow configuration creates a complex thermal interaction system characterized by multiple heat transfer mechanisms and time-dependent temperature distributions.

The temporal evolution of the wellbore temperature profile, illustrated in **Figure 6**, reveals several distinct thermal behavior regimes. During the initial circulation period (1-5 minutes), the temperature profile shows a sharp contrast between the cooler drilling fluid descending through the drill pipe and the warmer formation temperature. The heat transfer during this phase is dominated by conductive exchange through the drill pipe wall, where the temperature difference between the injected fluid and the annular fluid drives rapid thermal transport. As circulation progresses (5-20 minutes), a more complex temperature distribution develops. The annular fluid temperature profile exhibits a characteristic S-shaped curve, with three distinct zones: a lower zone where the fluid temperature approaches the formation temperature, a transition zone characterized by steep temperature gradients, and an upper zone where the temperature begins to stabilize. This profile shape results from the competing effects of advective heat transport by the flowing fluid and conductive heat exchange with the formation. A critical phenomenon emerges at approximately 20 minutes into the circulation when the temperature profile intersects the boiling point curve in the upper section of the wellbore. This intersection marks the onset of wellbore flashing, where the local fluid temperature exceeds the pressure-dependent boiling point. The physical mechanism driving this behavior can be attributed to the reduced hydrostatic pressure in the upper wellbore combined with the accumulated thermal energy transported from deeper sections.

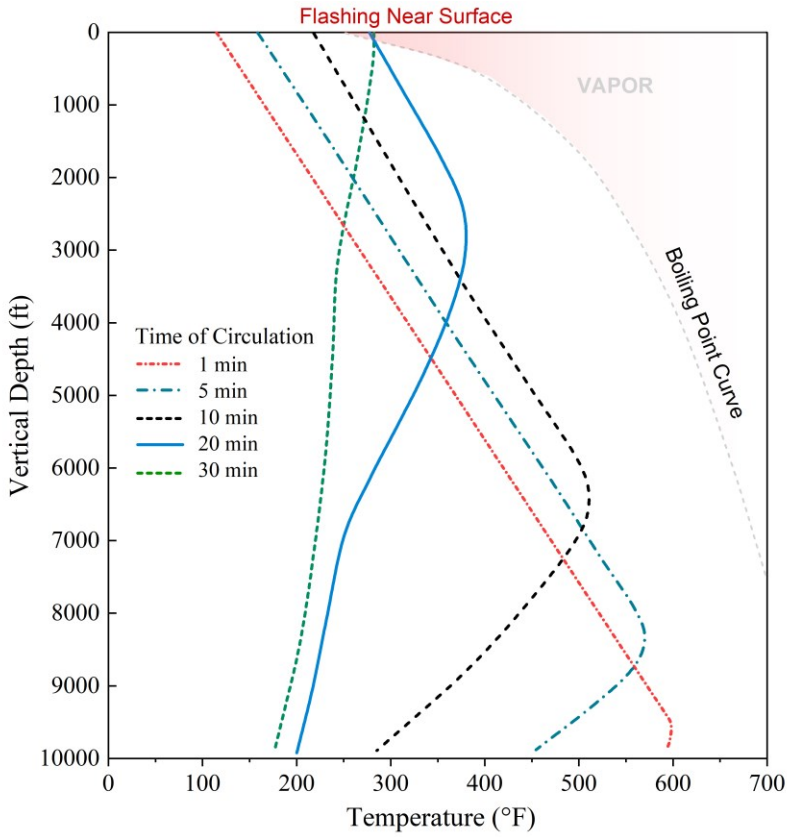

Figure 6. Wellbore fluid temperature profile with time and boiling point curve at wellbore conditions with 900gpm flow rate

The temperature profiles from 20-30 minutes demonstrate the progressive development of the flashing zone. The region where the fluid temperature exceeds the boiling point curve expands both vertically and in magnitude, indicating an increasing potential for vapor formation. This behavior is particularly significant in the uppermost 2000 feet of the wellbore, where the hydrostatic pressure is insufficient to suppress vapor formation at elevated temperatures. The boiling point curve (shown in orange) serves as a critical threshold, delineating the thermodynamic conditions where phase transition becomes possible. The increasing deviation between the fluid temperature profiles and this curve in the upper wellbore sections indicates a growing thermodynamic driving force for vapor generation. This deviation is most pronounced in the final temperature profile (30 minutes), suggesting that the system has not yet reached a steady state and that the flashing zone may continue to evolve.

The spatial variation in temperature gradients provides insight into the heat transfer mechanisms dominating different wellbore sections. The relatively flat temperature profile in the lower wellbore indicates near-equilibrium conditions with the formation, while the steeper gradients in the middle section reflect active heat transport processes. The complex temperature distribution in the upper section, where flashing occurs, results from the interplay between phase change thermodynamics, fluid dynamics, and heat transfer mechanisms.

This analysis demonstrates that the onset of wellbore flashing is not merely a local phenomenon but rather the result of integrated thermal-hydraulic processes throughout the wellbore system. The time-dependent evolution of temperature profiles suggests that careful consideration must be given to circulation parameters, particularly in the initial stages of operation, to manage the risk of unwanted phase transitions and their associated operational challenges.

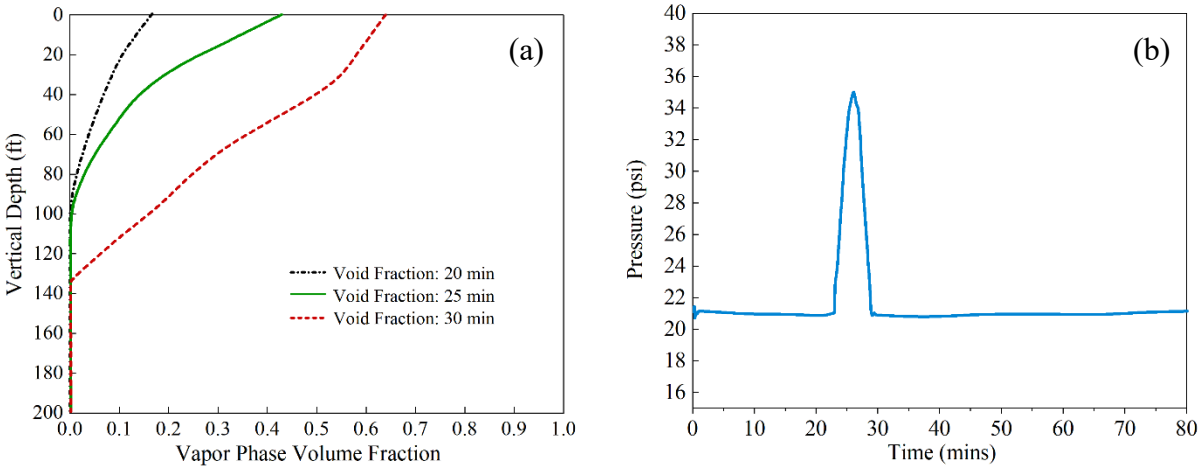

Figure 7. (a) – Vapor-phase volume fraction distribution along the top 140ft of the wellbore annulus at different times; (b) – Surface casing pressure versus time during initial circulation

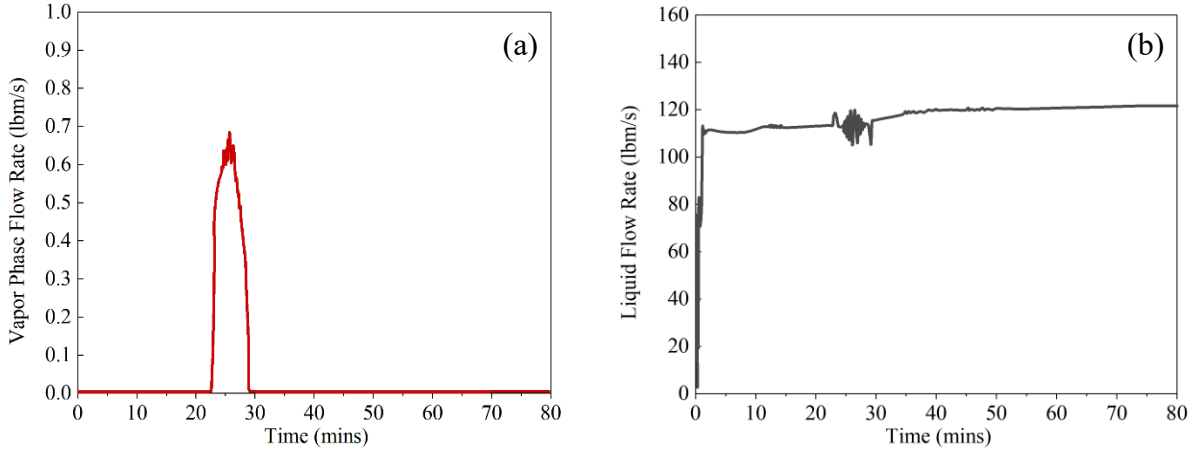

Figure 8. (a) – Vapor phase discharge rate on the surface versus time (b) – Liquid phase outflow rate on the surface versus time

The evolution of wellbore flashing is further illustrated in **Figure 7** and **Figure 8**. As shown in **Figure 7**(a), the model is able to capture the progressive formation and growth of steam (vapor) volume fraction in the uppermost 140 ft of the annulus over time. At 20 minutes, only a small amount of vapor is observed near the top of the wellbore, corresponding to the moment when the local fluid temperature first exceeds the saturation temperature at reduced annular pressure. By 25 minutes, the steam-filled region expands significantly downward, reflecting ongoing vapor generation as hot fluid continues to ascend. At 30 minutes, the void fraction profile indicates that a large portion of the top 140 ft has transitioned to a predominantly vapor-filled zone, reinforcing the observation that the flashing front continues to move downward until pressures and temperatures redistribute.

Figure 7 (b) highlights the effect of this vapor discharging on the surface casing pressure. Initially, the pressure remains steady, indicative of single-phase liquid flow. As soon as appreciable steam formation begins (near 20–25 minutes), a sharp pressure spike is observed, caused by the rapid evolution of vapor in the annulus and significant frictional pressure. This brief rise is then followed by a return toward a stabilized level, once the formed vapor discharges from the wellbore and the system adjusts to a two-phase flow regime.

The non-equilibrium phase-change modeling is further validated by the transient surface outflow rates shown in **Figure 8**. In **Figure 8 (a)**, the gas (vapor) flow rate at the surface remains negligible until the flashing zone advances enough for steam to reach the wellhead. A pronounced spike in vapor flow then appears between roughly 20 and 30 minutes, mirroring the timing of the casing-pressure increase. **Figure 8 (b)** shows that, during this same interval, the liquid outflow undergoes temporary fluctuations as a portion of the flow volume is replaced by vapor. After the steam "slug" passes through the wellhead, the liquid rate gradually returns to near its initial value, reflecting a transition to a less dramatic two-phase outflow.

Overall, these results demonstrate how flashing in geothermal wells—particularly after a lengthy shut-in period—can unfold rapidly once the annulus pressure falls below the local saturation pressure. The modeling approach captures all key aspects of the phenomenon: the spatial expansion of the vapor zone, the transient spike in surface casing pressure, and the simultaneous shifts in gas and liquid outflow. These consistent trends underscore the simulator's capacity for accurately tracking phase changes under strongly transient, high-enthalpy conditions. More importantly, the findings highlight the need to consider flashing onset when restarting circulation in hot geothermal

wells, emphasizing how the management of flow rate, pressure, and temperature gradients can be crucial in mitigating operational disturbances.

4. SENSITIVITY ANALYSIS AND MITIGATION STRATEGIES

The previous sections highlight how wellbore flashing can arise from a complex interplay of thermal-hydraulic processes once circulation restarts in a high-temperature geothermal well. Having established a robust baseline model of these dynamics, the next logical step is to systematically explore how various operational parameters and well characteristics influence both the onset and severity of flashing. By performing a series of sensitivity analyses, it becomes possible to pinpoint which parameters exert the greatest control over phase transition behaviors, thereby offering valuable insight into where mitigation efforts should be most strongly directed.

In this section, we examine key factors such as shut-in time, circulation rate, geothermal gradient, and well depth, quantifying their impact on transient temperature profiles and phase behavior. These parameters not only govern the thermodynamic conditions that give rise to flashing but also determine how quickly and how extensively vapor forms within the wellbore. The sensitivity studies aim to shed light on threshold conditions—those operational "tipping points" beyond which flashing events become especially rapid or large in magnitude.

Building on the findings of these parametric investigations, we then propose several mitigation strategies to minimize the operational and safety risks associated with flashing. By controlling circulation rates, managing wellbore pressures, and adjusting well design features, operators can reduce the likelihood of an abrupt phase transition or at least moderate its effects once it does occur. The recommended techniques, evaluated through complementary numerical simulations, provide a framework for more stable and efficient geothermal well operations in high-enthalpy environments.

4.1 Mud Circulation Rate

To examine the effect of mud circulation rate, simulations were conducted at varying flow rates, and the temperature profile near the surface was plotted over time, as shown in **Figure 9**. Notably, as the flow rate decreases, the peak temperature also decreases. This trend confirms that flow rate plays a crucial role in mitigating the risk of wellbore flashing. At higher flow rates, heat is transported more efficiently, leading to a steeper temperature rise and an earlier peak. Conversely, at lower flow rates, the heated fluid takes longer to reach the surface, causing a delayed peak in the temperature profile. The shift in peak temperature timing reflects the residence time of the fluid within the annulus, where slower-moving fluid has more time to transfer heat to the surrounding wellbore before reaching the surface. This further emphasizes the importance of optimizing circulation rates to control wellbore thermal conditions and prevent overheating that could trigger flashing.

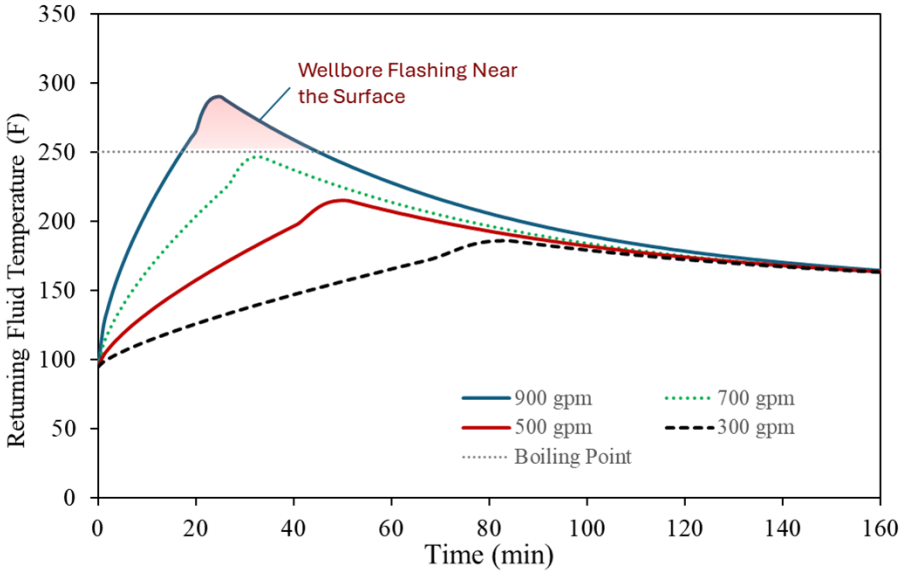

Figure 9. Effect of Circulation Rate on Annular Fluid Temperature Near the Surface

4.2 Well Total Depth

A sensitivity study was conducted to assess the impact of well depth on the rise of annular water temperature near the surface. A well with a depth of 5000 ft was simulated using a water circulation rate of 900 GPM while keeping all other parameters constant. As shown in **Figure 10**, the peak surface temperature for the shallower well is significantly lower than that of the deeper well.

This difference arises from two key factors. First, in a deeper well, the circulating fluid spends more time in contact with the high-temperature formation, allowing for greater heat absorption. The longer residence time and extended travel path result in a more substantial temperature rise before the fluid reaches the surface. Second, deeper wells inherently encounter higher geothermal gradients, leading to

much hotter fluid at the bottom section. This elevated initial temperature means that as the fluid ascends, it carries more thermal energy compared to a shallower well, where the bottom-hole temperature is considerably lower.

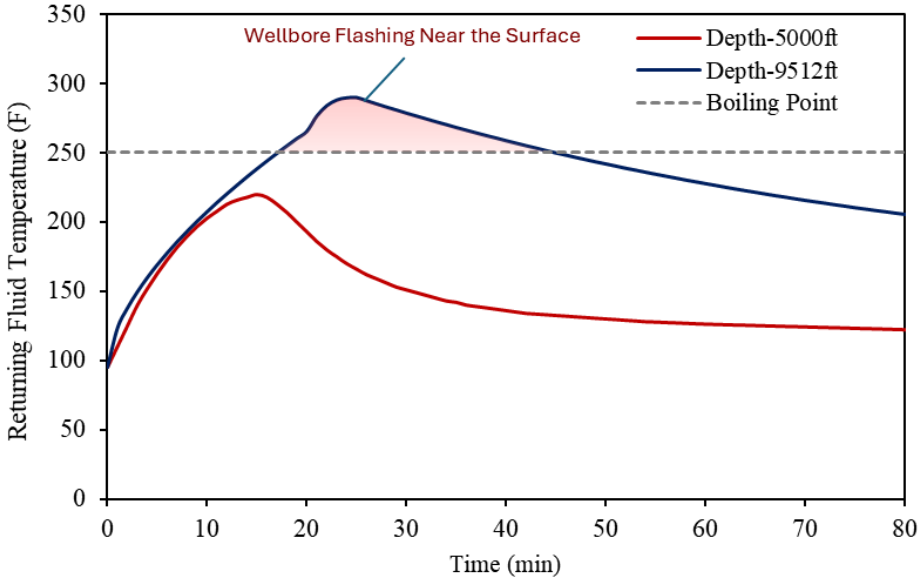

Figure 10. Effect of Well Depth on Annular Fluid Temperature Near the Surface

4.3 Geothermal Gradient

A sensitivity study was conducted to evaluate the impact of geothermal gradient on the annular fluid temperature near the surface. Two cases were simulated, one with a geothermal gradient of 3.3°F per 100 ft and another with a higher gradient of 5.2°F per 100 ft, while keeping all other parameters constant. **Figure 11** illustrates the resulting temperature profiles.

The results indicate that a higher geothermal gradient leads to a significantly higher peak temperature at the surface. This occurs because a steeper geothermal gradient means that the formation temperature is higher at every depth, resulting in hotter fluid at the bottom of the well. As the fluid circulates, it carries this additional thermal energy upward, leading to an overall increase in temperature throughout the system. In contrast, with a lower geothermal gradient, the formation temperature is relatively lower, limiting the amount of heat absorbed by the circulating fluid and leading to a reduced peak temperature.

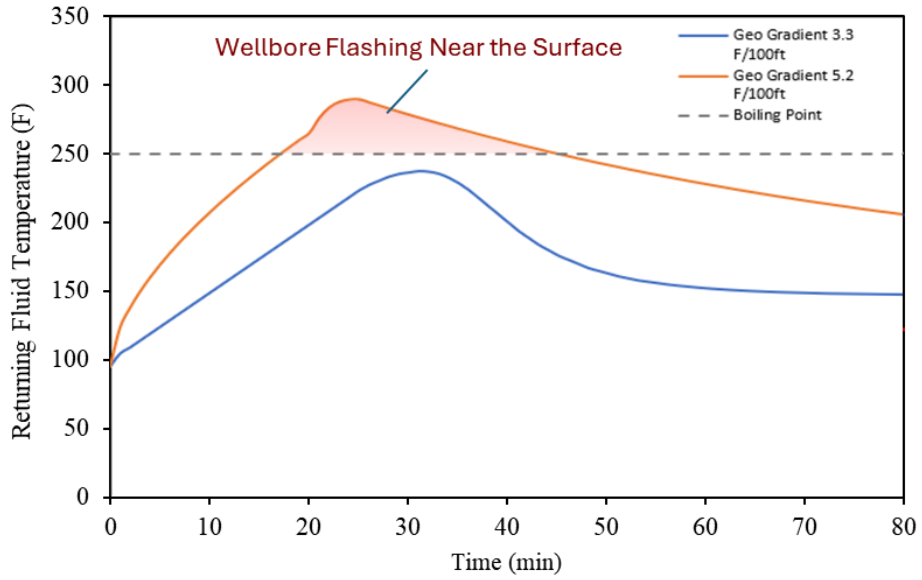

Figure 11. Effect of Geothermal Gradient on Annular Fluid Temperature Near the Surface

Additionally, the time at which the peak temperature occurs is slightly delayed in the lower geothermal gradient case. This is because the rate of heat accumulation is lower, requiring more time for the circulating fluid to reach its maximum temperature. Importantly, the higher gradient case surpasses the boiling point threshold, increasing the likelihood of flashing and steam formation, whereas the lower gradient case remains below this critical point.

4.4 Shut-in Period

A sensitivity analysis was conducted to examine the effect of varying shut-in periods on the annular fluid temperature near the surface during subsequent circulation. Simulations were performed using a circulation rate of 900 GPM, with different shut-in durations before resuming circulation. The well is assumed to have been continuously circulated for extended periods of time, and a near steady-state heat transfer has been established. The black curves in **Figure 12** illustrate the estimated near steady-state temperature profiles obtained from the developed transient heat transfer simulator. Afterward, the well is assumed to be shut in with no circulation. The simulator is then used to estimate how the temperature profile evolves over time during these idle periods. The curves in **Figure 12** demonstrate the temperature distributions after 6 hours, 24 hours, 3 days, 10 days, and 20 days of non-circulation.

A comparison of the temperature curves confirms that even relatively short shut-in durations allow the fluid column to warm significantly, particularly near the bottom of the well. After only 6 hours of non-circulation, the lower intervals show a noticeable upward shift in temperature relative to the steady-state baseline. This reflects the cessation of advective cooling that was otherwise maintained under continuous circulation. Prolonged shut-in times—24 hours or more—allow the deeper sections of the wellbore fluid to approach the local geothermal temperature. As a result, the net temperature difference between the bottomhole region and the upper wellbore grows more pronounced with each additional day of downtime.

These increasingly elevated bottomhole temperatures, combined with the larger temperature gradient in the upper sections, have direct implications for wellbore flashing once circulation restarts. When a well resumes pumping at 900 GPM after, for instance, a 10- or 20-day shut-in, the hot fluid column that has equilibrated with the formation is suddenly forced upward. Because the hydrostatic pressure near the surface is lower, the temperature at which the fluid can flash into vapor drops accordingly, making it more likely that portions of the upward-moving fluid will cross the local saturation envelope. Longer idle periods thus translate into a greater stored thermal load within the wellbore, ultimately raising both the likelihood and the intensity of flashing events.

Operationally, these results emphasize the importance of carefully planning shut-in strategies in high-enthalpy geothermal wells. If extended downtime is unavoidable—due, for instance, to equipment maintenance or unplanned operational delays—operators may need to implement additional measures such as staged re-circulation ramp-ups or pre-circulation cooling treatments to mitigate the risk of encountering severe two-phase flow conditions. By tailoring shut-in durations, monitoring bottomhole temperatures, and managing circulation rates during re-start, significant improvements in well stability and overall system reliability can be achieved.

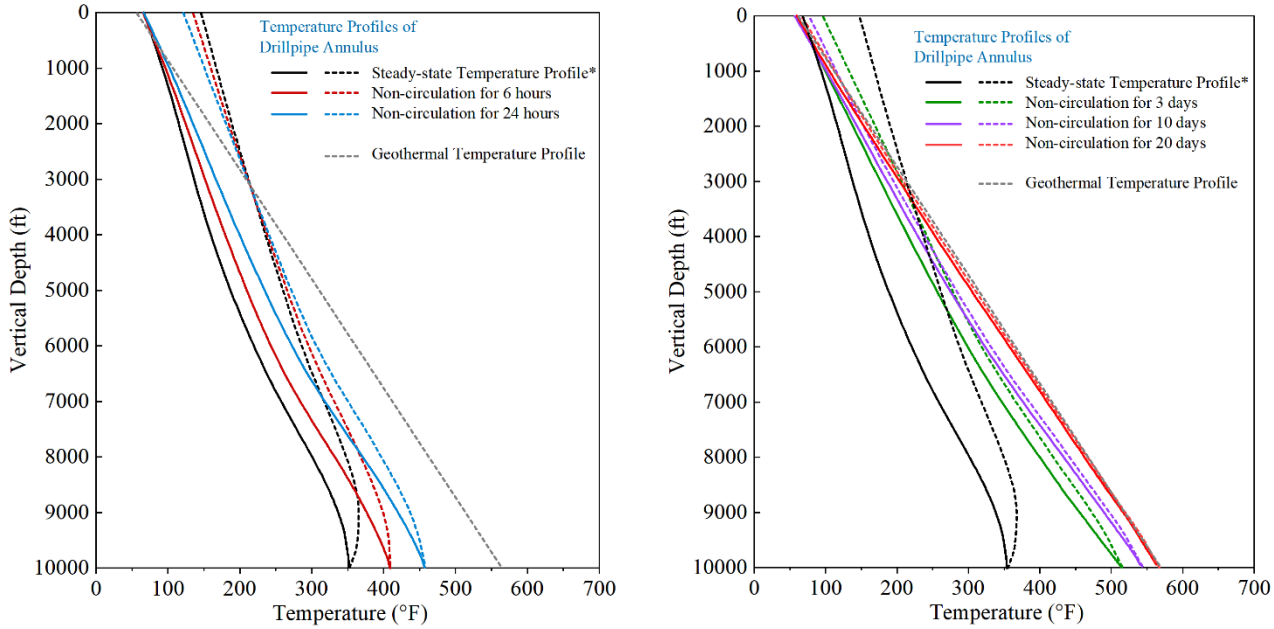

* The Temperature Profiles after the Well is Continuously Circulated for 20 days, Estimated Using the Developed Transient Heat Transfer Simulator

Figure 12. Estimated Wellbore Fluid Temperature Profiles after Different Times of Non-circulation

Figure 13 illustrates the temperature profiles over time for varying shut-in periods and their effect on fluid temperatures during subsequent circulation. The data demonstrates that longer shut-in periods result in progressively higher peak temperatures in the wellbore fluid when circulation resumes. This increase occurs because, during the shut-in period, heat from the surrounding formation continually transfers into the stagnant wellbore fluid. The longer the fluid remains static, the more thermal energy it accumulates, raising its initial temperature before re-starting circulation. As the shut-in duration increases, the wellbore fluid temperatures begin to approach the local geothermal temperature, especially at depth. When circulation is eventually resumed, the fluid starts at these elevated temperatures, which leads to higher temperatures in the returning flow compared to scenarios with shorter non-circulation periods. This buildup of heat presents

a critical operational concern: the fluid in the wellbore may exceed its local boiling point under lower pressure conditions near the surface, making flashing more prone to occur. In extreme cases, the peak temperature profiles surpass the local boiling point curve for the fluid, potentially triggering two-phase flow and associated operational challenges. The implications of these findings underscore the importance of managing shut-in durations carefully in geothermal systems. Longer shut-ins not only store more heat in the wellbore but also increase the likelihood of flashing when circulation restarts. To mitigate such risks, strategies such as pre-circulation cooling or staged ramp-ups in circulation rate may be required in long downtime instances to minimize the severity of temperature spikes and prevent flashing from affecting wellbore stability and flow consistency. for 16 seconds

As shown by **Figure 13**, the returning annular fluid temperature over time for a range of shut-in durations, from 6 hours to 20 days, once circulation is resumed at 900 GPM. The results show that longer downtime corresponds to higher peak temperatures in the produced fluid. During non-circulation, heat continuously flows from the surrounding formation into the stagnant wellbore fluid; the longer this idle period, the more extensively the fluid equilibrates toward the elevated geothermal temperature at depth. Consequently, when pumping restarts, the returning fluid begins at a higher initial temperature and reaches a more pronounced peak before cooler fluid from the surface fully displaces the heated column. Notably, some curves exceed the local boiling point, underscoring the increased risk of flashing after extended shut-in periods. Eventually, all temperature curves converge downward as the cooler circulation fluid flushes out the hotter volumes from the deep wellbore, but the timing and severity of any flash event depend on both the maximum temperature reached and the local pressure conditions in the upper annulus.

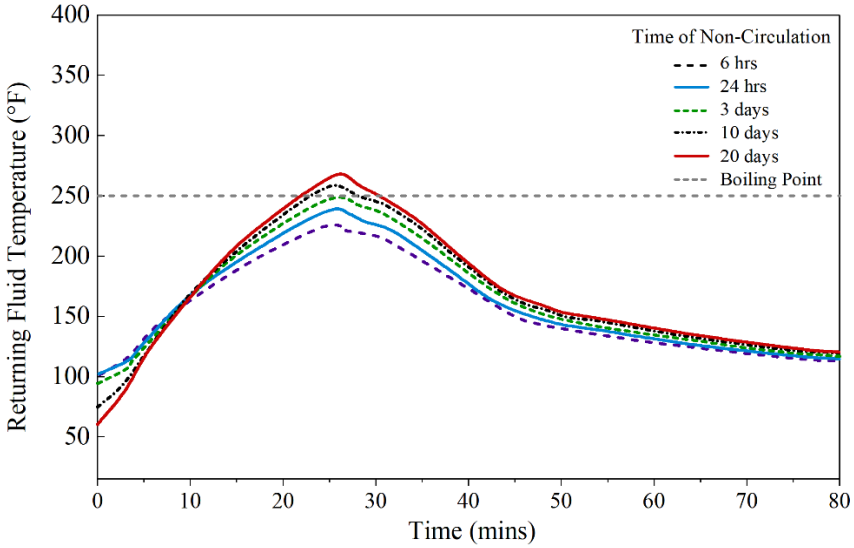

Figure 13. Effect of Shut-in Duration on Annular Fluid Temperature and Flashing Risk During Circulation

4.5 Discussion on Flashing Mitigation Strategies during Initial Circulation after Prolonged Non-circulation

Effective management of transient thermal and pressure conditions is key to mitigating wellbore flashing during the critical period of restarting circulation after a prolonged shut-in. As demonstrated in the preceding analyses, flashing typically occurs when the local fluid temperature exceeds the saturation temperature at a given pressure—most often in the upper sections of the wellbore where hydrostatic pressure is reduced. By tackling both the rate at which heat is transported from deeper zones and the local wellbore pressures, operators can curb the rapid onset of vapor formation and thereby reduce equipment strain, surface pressure spikes, and two-phase flow instabilities.

A primary mitigation strategy is the gradual increase of circulation rate, particularly in the first few minutes of pumping after a long shut-in. By ramping up circulation slowly rather than instantly jumping to the final pump rate, the system experiences a smoother transition in both temperature and pressure. This not only helps dissipate a portion of the accumulated heat but also allows time for any incipient vapor bubbles to collapse or exit the wellbore before they grow into significant volumes. Numerical simulations confirm that high pumping rates can help cool the upper annulus more rapidly but, if applied abruptly, can create strong local pressure drops and inadvertently trigger flashing in the near-surface region.

Pressure management through backpressure control or managed-pressure drilling (MPD) technology is another potent tool for preventing flash events. By maintaining an annular pressure slightly above the critical saturation threshold, operators can effectively “push down” the boiling point curve, keeping the fluid in the liquid phase for a longer vertical interval. This approach is especially valuable in high-enthalpy wells with a limited margin between static formation temperature and the saturation temperature for the circulation fluid.

Where operationally viable, pre-circulation cooling can also ease flashing risks. Circulating a cooler fluid at a very low rate immediately before the full circulation gradually absorbs and removes heat from the near-wellbore region without causing abrupt pressure transients. Although this method may extend rig time, it can be particularly effective in situations where reservoir permeability is low and heat accumulation in the wellbore is extensive.

Finally, wellbore design considerations—such as using insulated drill pipe or specialized casing materials—can reduce radial heat

transfer from formation to fluid, thereby lowering the likelihood that temperature in the annulus will climb to flashing thresholds. As illustrated by the simulations case studies in this research, small changes in thermal resistance can produce significant shifts in local fluid-temperature profiles, delaying or preventing the intersection of fluid temperature with the boiling-point curve.

In summary, a combination of careful pump-rate ramp-up, active pressure control, selective pre-circulation cooling, and strategic wellbore design choices afford the best protection against flash events when re-establishing circulation in hot geothermal wells. The numerical modeling insights reinforce that even modest operational changes can markedly diminish the severity of pressure spikes and two-phase outflow, ultimately supporting more reliable and safer geothermal drilling.

5. CONCLUSIONS AND FUTURE WORK

This study introduces a comprehensive modeling approach to simulate phase change behavior during the initial circulation phase following extended non-circulation periods, during which elevated wellbore temperatures prevail. Advanced numerical simulations are employed to analyze transient fluid flow and heat transfer dynamics, while the modeling framework incorporates non-equilibrium phase change relaxation models to capture delayed phase transitions.

Numerical simulations indicate that as the formation-heated fluid with high-temperature ascends during the initial circulation after pro-longed non-circulation, the reduction in hydrostatic pressure markedly increases the risk of vaporization and potential wellbore flashing. The integrated modeling framework, which couples non-equilibrium phase change relaxation with detailed transient heat transfer analysis, reveals that sharp thermal gradients along the drill pipe and annulus—particularly in the upper wellbore—combine with rapid pressure drops to create localized conditions favorable for significant vapor formation. Detailed analysis of base cases shows that during the initial circulation phase, the abrupt change in thermal and pressure profiles drives the fluid state past its saturation threshold, thereby initiating flashing. Sensitivity analyses further indicate that key operational parameters, such as circulation rate, well depth, geothermal gradient, and shut-in duration, substantially influence both the risk and intensity of flashing. In particular, extended shut-in periods and elevated geothermal gradients lead to pronounced thermal loading, which reduces the pressure margin for maintaining a liquid phase, leading to higher likelihood of triggering unwanted phase transitions and wellbore flashing events.

In light of these findings, the study has proposed several mitigation strategies aimed at enhancing operational safety and efficiency. Gradual ramp-up of circulation rates, coupled with effective pressure management techniques, can help dissipate accumulated heat and maintain the wellbore fluid below critical flashing thresholds. Additionally, the potential benefits of pre-circulation cooling and improved wellbore insulation were highlighted as promising avenues for reducing thermal influx from the formation. These operational adjustments, when implemented in conjunction with real-time monitoring, offer a practical pathway to mitigate the risks associated with sudden flashing events.

This research provides valuable insights into the dynamics of the thermal and hydraulic processes in geothermal wellbores, establishing a foundation for future advancements in geothermal drilling operations. The integrated modeling approach advances our understanding of flashing mechanisms and offers actionable strategies to control and mitigate its adverse effects. As the geothermal industry continues to expand, the insights derived from this work will be instrumental in guiding the design of safer, more reliable, and more efficient geothermal energy extraction systems.

Future research should focus on validating the presented modeling framework against additional field data drawn from two‐phase flow conditions in high‐enthalpy geothermal systems such as Utah FORGE, thereby bolstering confidence in both the thermodynamic and fluid‐dynamic aspects of the simulations. Concurrently, further investigation into optimized operational guidelines to prevent or mitigate flashing is warranted. This includes examining controlled circulation ramp-up protocols, precise pressure management techniques, and pre-circulation cooling strategies. Such studies will not only refine the predictive capabilities of the current model but also contribute to developing robust mitigation strategies that enhance wellbore stability and overall operational safety in geothermal energy extraction.

ACKNOWLEDGEMENT

This research is supported and funded by the Department of Energy (DOE) Geothermal Technologies Office (GTO) through the Geothermal Limitless Approach to Drilling Efficiencies (GLADE) project (Grant No. DE-EE0010444) led by Oxy USA, Inc. The authors would like to acknowledge Idaho National Laboratory (INL) for providing access to the RELAP5-3D software platform and computational resources.

REFERENCES

Abdelhafiz, M. M., et al. (2021). "Temperature modeling for wellbore circulation and shut-in with application in vertical geothermal wells." Journal of petroleum science and engineering 204: 108660.

Adeyemi, Temitayo, et al. "Comparison of Gas Signature and Void Fraction in Water-and Oil-Based Muds Using Fiber-Optic Distributed Acoustic Sensor, Distributed Temperature Sensor, and Distributed Strain Sensor." SPE Journal (2024): 1-22.

Adityatama, D. W., et al. (2020). Slimhole Drilling Overview for Geothermal Exploration in Indonesia: Potential and Challenges.

Adrian, A., et al. (2015). A simplified transient multi-phase model for automated well control applications. International Petroleum Technology Conference, Doha, Qatar.

Akasaka, C., et al. (2011). "A large wellfield steam explosion at the Onikobe Geothermal power station." GRC Trans 35: 1221-1226.

Akbar, S., Fathianpour, N., & Khoury, R. (2016). A finite element model for high enthalpy two-phase flow in geothermal wellbores. Renewable Energy, 94, 223-236. https://doi.org/10.1016/j.renene.2016.03.034

Ambrus, A., et al. (2016). "Real-time estimation of reservoir influx rate and pore pressure using a simplified transient two-phase flow model." Journal of Natural Gas Science and Engineering 32: 439-452.

Arista, J. A. R., et al. (2022). Exploring the Use of Temperature Transient Analysis During Pressure Falloff Testing in Geothermal Wells. Proceedings 44th New Zealand Geothermal Workshop.

Avelar, C. S., et al. (2009). "Deepwater gas kick simulation." Journal of petroleum science and engineering 67(1-2): 13-22.

Bahonar, M., et al. (2010). "A semi-unsteady-state wellbore steam/water flow model for prediction of sandface conditions in steam injection wells." Journal of Canadian Petroleum Technology 49(09): 13-21.

Bayutika, I. G. (2018). Geothermal Well Control & Momentum Kill Equation for Surface Bullheading.

Bird, R., et al. (2002). "Transport Phenomena, John Wiley & Sons, New York, NY, USA."

Bourgoyne Jr, A. (1989). Experimental study of erosion in diverter systems due to sand production. SPE/IADC Drilling Conference and Exhibition, SPE.

Brown, C. A., et al. (2023). Enablement of High-Temperature Well Drilling for Multilateral Closed-Loop Geothermal Systems. Proceedings: 48th Workshop on Geothermal Reservoir Engineering, Stanford University, Stanford, California.

Canbaz, C., Ekren, O., & Aksoy, N. (2022). Review of wellbore flow modelling in co2-bearing geothermal reservoirs. Geothermics, 98, 102284. https://doi.org/10.1016/j.geothermics.2021.102284

Chadha, P., et al. (1993). "Modelling of two-phase flow inside geothermal wells." Applied mathematical modelling 17(5): 236-245.

Chen, X., et al. (2021). The Challenge of Elastomer Seals for Blowout Preventer BOP and Wellhead/Christmas Trees under High Temperature. Offshore Technology Conference.

Clauser, C. and E. Huenges (1995). Rock Physics and Phase Relations. A Handbook of Physical Constants. 3: 105-126.

Cole, P., et al. (2017). Geothermal drilling: a baseline study of nonproductive time related to lost circulation. Proceedings of the 42nd Workshop on Geothermal Reservoir Engineering, Stanford, CA, USA.

Corre, B., et al. (1984). Numerical Computation of Temperature Distribution in a Wellbore While Drilling. SPE Annual Technical Conference and Exhibition.

Deligiannis, P. and J. Cleaver (1992). "The influence of critical bubble swarms on the rate of nucleation." Chemical engineering science 47(12): 3142-3144.

Delong, Z., et al. (2014). "Study on Well Control Technology of High Temperature Geothermal Drilling." Procedia Engineering 73: 337-344.

DiPippo, R. (2016). Geothermal Power Plants: Principles, Applications, Case Studies and Environmental Impact (4th ed.). Butterworth-Heinemann.

Dirker, J. and J. P. Meyer (2005). "Convective heat transfer coefficients in concentric annuli." Heat Transfer Engineering 26(2): 38-44.

Falavand-Jozaei, A., et al. (2022). "Modeling and simulation of non-isothermal three-phase flow for accurate prediction in underbalanced drilling." Petroleum Exploration and Development 49(2): 406-414.

Fatemeh, K., et al. (2020). "Geothermal Drilling: A Review of Drilling Challenges with Mud Design and Lost Circulation Problem."

Feder, J. (2021). "Geothermal well construction: a step change in oil and gas technologies." Journal of Petroleum Technology 73(01): 32-35.

Finger, J. T. and D. A. Blankenship (2012). Handbook of best practices for geothermal drilling, Sandia National Lab.(SNL-NM), Albuquerque, NM (United States).

Forouzanfar, F., et al. (2015). Formulation of a transient multi-phase thermal compositional wellbore model and its coupling with a thermal compositional reservoir simulator. SPE Annual Technical Conference and Exhibition, SPE.

Frank, T. (2005). Advances in computational fluid dynamics (CFD) of 3-dimensional gas-liquid multiphase flows. NAFEMS Seminar: Simulation of Complex Flows (CFD)–Applications and Trends, Wiesbaden, Germany, Citeseer.

Gabaldon, Oscar, et al. "Expanded IME with New Riser Gas Handling Operation Region." SPE/IADC Managed Pressure Drilling and Underbalanced Operations Conference and Exhibition. SPE, 2022.

García-Valladares, O., et al. (2006). "Numerical modeling of flow processes inside geothermal wells: An approach for predicting

production characteristics with uncertainties." Energy Conversion and Management 47(11-12): 1621-1643.

Ghobadpouri, S., et al. (2017). "Modeling and simulation of gas-liquid-solid three-phase flow in under-balanced drilling operation." Journal of petroleum science and engineering 156: 348-355.

Grace, R. D., et al. (2003). "Blowout and well control handbook." Blowout and Well Control Handbook: 1-469.

Hasan, A. R. and C. S. Kabir (2010). "Modeling two-phase fluid and heat flows in geothermal wells." Journal of petroleum science and engineering 71(1-2): 77-86.

Huan, X., Xu, G., Zhang, Y., Sun, F., & Xue, S. (2021). Study on thermo-hydro-mechanical coupling and the stability of a geothermal wellbore structure. Energies, 14(3), 649. https://doi.org/10.3390/en14030649

Izuwa, N. (2024). Modeling of wellbore heat transfer in geothermal production well. Iop Conference Series Earth and Environmental Science, 1342(1), 012041. https://doi.org/10.1088/1755-1315/1342/1/012041

Lei, H., Xie, Y., Li, J., & Hou, X. (2023). Modeling of two-phase flow of high-temperature geothermal production wells in the yangbajing geothermal field, tibet. Frontiers in Earth Science, 11. https://doi.org/10.3389/feart.2023.1019328

Martinez-Galvan, E., et al. (2016). "Numerical Simulation of Two-Phase Flow in Geothermal Wells Using RELAP5-3D." Geothermics, 65, 120-134.

Mohammadi, S. (2024). Analysis of transient heat transfer in geothermal engineering: effect of seasonal fluctuations in ates systems. https://doi.org/10.21203/rs.3.rs-5246201/v1

Nwaka, Nnamdi, Chen Wei, and Yuanhang Chen. "A simplified two-phase flow model for riser gas management with non-aqueous drilling fluids." Journal of Energy Resources Technology 142.10 (2020): 103001.

Nwaka, Nnamdi, et al. "Gas in riser: On modeling gas influxes in non-aqueous drilling fluids with time-dependent desorption considerations." Journal of Petroleum Science and Engineering 195 (2020): 107785.

Perry, Scott, Chen Wei, and Yuanhang Chen. "Absorption kinetics of gas influxes into nonaqueous fluids during riser gas handling events." AADE 2020 Fluids Technical Conference, Marriott Marquis, Houston, Texas. 2020.

Shimizu, Y., Morita, S., & Kumano, H. (2019). "Analysis of Two-Phase Flow Dynamics in Geothermal Wells During Start-up Operations." Geothermics, 82, 7-18.

Tabjula, Jagadeeshwar L., et al. "Well-scale experimental and numerical modeling studies of gas bullheading using fiber-optic DAS and DTS." Geoenergy Science and Engineering 225 (2023): 211662.

Tester, J. W., Drake, E. M., Driscoll, M. J., Golay, M. W., & Peters, W. A. (2021). Sustainable Energy: Choosing Among Options (3rd ed.). MIT Press.

Watson, A., Malin, P. E., & Foulger, G. R. (2020). "Recent Advances in Modeling Transient Phenomena in Geothermal Wells." Journal of Volcanology and Geothermal Research, 390, 106768.

Wei, Chen, and Yuanhang Chen. "A study of the fixed choke and constant outflow method for riser gas handling." Process Safety and Environmental Protection 174 (2023): 756-769.

Wei, Chen, and Yuanhang Chen. "On improving algorithm efficiency of gas-kick simulations toward automated influx management: a Robertson differential-algebraic-equation problem approach." SPE Drilling & Completion 36.04 (2021): 943-966.

Wei, Chen, et al. "An Evaluation of Pressure Control Methods During Riser Gas Handling with MPD Equipment Based on Transient Multiphase Flow Modeling and Distributed Fiber Optic Sensing." SPE Annual Technical Conference and Exhibition. SPE, 2022.

Wei, Chen, et al. "Full-scale experimental and modeling studies of gas migration and suspension behaviors during wellbore influx management using MPD." SPE Annual Technical Conference and Exhibition. SPE, 2023.

Wei, Chen, et al. "Improved gas influx distribution estimation using interfacial area transport equation (IATE) enabled two-fluid model: An advanced modeling and full-scale experimental study." International Journal of Multiphase Flow 172 (2024): 104706.

Wei, Chen, et al. "The modeling of two-way coupled transient multiphase flow and heat transfer during gas influx management using fiber optic distributed temperature sensing measurements." International Journal of Heat and Mass Transfer 214 (2023): 124447.

Zhao, W. (2023). Heat production performance from an enhanced geothermal system (egs) using co2 as the working fluid. Energies, 16(20), 7202. https://doi.org/10.3390/en16207202